© 2017. Published by The Company of Biologists Ltd | Development (2017) 144, 3315-3324 doi:10.1242/dev.149765

RESEARCH ARTICLE

Differing contributions of the first and second pharyngeal arches to tympanic membrane formation in the mouse and chick

Toshiko Furutera[1,*], Masaki Takechi[1,*,‡], Taro Kitazawa[2,3,4], Junko Takei[1], Takahiko Yamada[1], Tri Vu Hoang[1], Filippo M. Rijli[4,5], Hiroki Kurihara[2,3,6], Shigeru Kuratani[7] and Sachiko Iseki[1]

ABSTRACT

We have proposed that independent origins of the tympanic membrane (TM), consisting of the external auditory meatus (EAM) and first pharyngeal pouch, are linked with distinctive middle ear structures in terms of dorsal-ventral patterning of the pharyngeal arches during amniote evolution. However, previous studies have suggested that the first pharyngeal arch (PA1) is crucial for TM formation in both mouse and chick. In this study, we compare TM formation along the anterior-posterior axis in these animals using *Hoxa2* expression as a marker of the second pharyngeal arch (PA2). In chick, the EAM begins to invaginate at the surface ectoderm of PA2, not at the first pharyngeal cleft, and the entire TM forms in PA2. Chick-quail chimera that have lost PA2 and duplicated PA1 suggest that TM formation is achieved by developmental interaction between a portion of the EAM and the columella auris in PA2, and that PA1 also contributes to formation of the remaining part of the EAM. By contrast, in mouse, TM formation is highly associated with an interdependent relationship between the EAM and tympanic ring in PA1.

KEY WORDS: Tympanic membrane, External auditory meatus, Middle ear, *Hoxa2*, Chick-quail chimera, Morphological evolution, Mouse

INTRODUCTION

The ear is divided into three anatomical compartments: the external, middle, and inner ear. The external ear consists of the external auditory meatus (EAM) and (only in mammals) the pinna, which collect sound. The inner ear contains the cochlea, a sensory organ for hearing that converts sound into neural pulses. The middle ear, which comprises the middle ear ossicle(s) and tympanic membrane (TM), amplifies air vibrations (sound) and transmits them to the inner ear. The morphology of the middle ear is highly associated with the lifestyle of terrestrial tetrapods (Clack and Allin, 2004; Wever, 1978). The mammalian middle ear has three ossicles: the malleus, incus, and stapes, whereas diapsids (modern reptiles and birds) have only one ossicle, the columella auris. Comparative morphological analyses have concluded that the incus and malleus have been derived from jaw-joint skeletal elements – the quadrate and articular elements, respectively – of a pre-mammalian ancestor (Anthwal et al., 2013; Maier and Ruf, 2016; Manley and Sienknecht, 2013; Reichert, 1837; Takechi and Kuratani, 2010). The stapes is homologous with the columella auris. Paleontological studies have suggested that the middle ear evolved independently several times in tetrapods (Clack, 2002; Laurin, 1998, 2010; Lombard and Bolt, 1979; Müller and Tsuji, 2007). However, precisely how this transformation from jaw-joint elements to middle ear ossicles took place has remained an intriguing question for many years.

The middle ear ossicles and TM are produced from all three germ layers, including the cranial neural crest cells (CNCCs) derived from the ectoderm, in the pharyngeal arches (PAs). The incus (or quadrate) and malleus (or articular) are mostly derived from CNCCs in the first pharyngeal arch (PA1), and the stapes (or columella auris) originates from CNCCs in the second pharyngeal arch (PA2) and from mesodermal cells (Köntges and Lumsden, 1996; Noden, 1986; Rijli et al., 1993; Thompson et al., 2012). The TM comprises three components both in mammals and diapsids: the external auditory meatus (EAM), which is derived from the surface ectoderm; the first pharyngeal pouch (PP1), which comprises the pharyngeal endoderm between PA1 and PA2; and fibrous mesenchymal cells (Chapman, 2011; Chin et al., 1997). The EAM and PP1 contact each other and form a thin layer, sandwiching the middle ear ossicle (Mallo, 2001, 2003). In the mouse, the EAM invaginates toward the forming tympanic ring, an intramembranous bone surrounding the EAM, and then contacts with PP1 to form the TM (Fig. 1A-C) (Mallo and Gridley, 1996; Mallo et al., 2000). The goosecoid (*Gsc*) knockout mouse exhibits loss of the EAM and tympanic ring, resulting in lack of the TM (Yamada et al., 1995). Therefore, development of the EAM and tympanic ring are considered to be interdependent in the mouse. Studies in mouse and chick have suggested that development of the middle ear requires histologically and molecularly coordinated interactions between the epithelium and mesenchyme in PA1 and PA2 (Fuchs and Tucker, 2015; Mallo, 2001, 2003; Takechi et al., 2016; Zou et al., 2012). Thus, the different patterns of the middle ears in mammals and diapsids should be ascribed to changes in the developmental programs for PA1 and PA2, and we consider that the evolutionary relationship between the TM and skeletal elements is key to solving morphological evolution of the middle ear in amniotes (Takechi and Kuratani, 2010; Kitazawa et al., 2015a).

Endothelin 1 (Edn1) signaling works as a selector of lower jaw development in jawed vertebrates (Clouthier et al., 2013; Medeiros

[1]Section of Molecular Craniofacial Embryology, Graduate School of Medical and Dental Sciences, Tokyo Medical and Dental University (TMDU), 1-5-45 Yushima, Bunkyo-ku, Tokyo 113-8549, Japan. [2]Department of Physiological Chemistry and Metabolism, Graduate School of Medicine, The University of Tokyo, 7-3-1, Hongo, Bunkyo-ku, Tokyo 113-0033, Japan. [3]Core Research for Evolutional Science and Technology (CREST), Japan Science and Technology Agency (JST), Chiyoda-ku, Tokyo, 102-0076, Japan. [4]Friedrich Miescher Institute for Biomedical Research, Affiliated to the Novartis Institutes for Biomedical Research, Maulbeerstrasse 66, CH-4058 Basel, Switzerland. [5]University of Basel, Petersplatz 10, 4003 Basel, Switzerland. [6]Institute for Biology and Mathematics of Dynamical Cell Processes (iBMath), The University of Tokyo, 3-8-1 Komaba, Meguro-ku, Tokyo 153-8914, Japan. [7]Evolutionary Morphology Laboratory, RIKEN, 2-2-3 Minatojimaminami-machi, Chuo-ku, Kobe, 650-0047, Japan.
*These authors contributed equally to this work

‡Author for correspondence (takechi.emb@tmd.ac.jp)

T.F., 0000-0002-3617-2360; M.T., 0000-0001-7279-9243

Received 25 January 2017; Accepted 4 August 2017

Development (2017) 144, 3315-3324 doi:10.1242/dev.149765

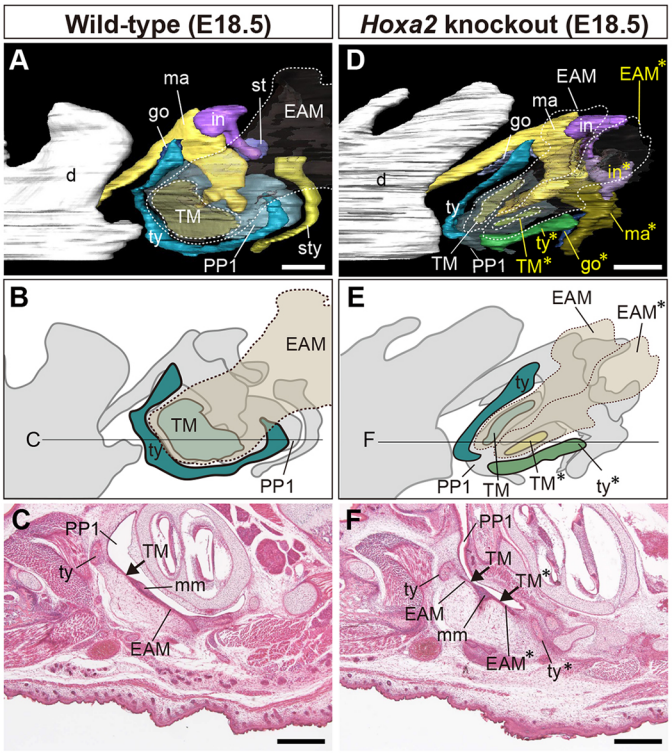

Fig. 1. The middle ear region of wild-type and *Hoxa2* knockout mice. 3D reconstruction of the middle ear in the E18.5 wild-type (A) and *Hoxa2* knockout (*Hoxa2*$^{EGFP/EGFP}$) (D) mouse in lateral view. Schematic drawings of the 3D reconstruction are shown for the wild-type (B) and *Hoxa2* knockout (E) mice, highlighting the tympanic ring, EAM and TM. (C,F) Horizontal section (Hematoxylin and Eosin staining) of the wild-type (C) and *Hoxa2* knockout (F) mouse in the planes indicated in B and Es. Asterisks mark duplicated structures. d, dentary; EAM, external auditory meatus; go, gonial bone; in, incus; ma, malleus; mm, manubrium of malleus; PP1, first pharyngeal pouch; st, stapes; sty, styloid process; TM, tympanic membrane; ty, tympanic ring. Scale bars: 500 µm.

and Crump, 2012). Inhibition of Edn1 signaling results in transformation of the lower jaw into an upper-jaw-like structure in mouse (Ozeki et al., 2004; Ruest et al., 2004; Sato et al., 2008) and chick (Kempf et al., 1998; Kitazawa et al., 2015a). We previously found that inhibition of Edn1 signaling causes loss of the TM in mouse, but its duplication in chick (Kitazawa et al., 2015a). Therefore, the TM is dependent on different mechanisms underlying developmental patterning along the dorsal-ventral axis; Edn1-dependent lower jaw formation influences TM formation in mammals, whereas Edn1-independent upper jaw formation is relevant to the diapsid TM (Kitazawa et al., 2015a). These results strongly suggest independent origins of the TM during amniote evolution. In other words, although the TM is formed by similar processes in both mammals and diapsids, the acquisition of the TM is likely to result from parallel evolution in these lineages. Thus, it is of interest to elucidate similarities and differences in the developmental mechanisms of the TM in the mammal and diapsid lineages to understand the genetic bases underlying this type of morphological evolution.

The positional specifications of PAs along the anterior-posterior (A-P) axis are mediated by a collinear, nested expression pattern of Hox genes in the CNCCs. No Hox genes are expressed in the CNCCs of PA1. By contrast, *Hoxa2* is expressed in the CNCCs of PA2 and more posterior regions of the body, and this gene expression is considered to provide the morphological identity of PA2. In *Hoxa2* knockout mice, the PA2-derived components are transformed into PA1 derivatives such as the malleus, incus and the tympanic ring (Fig. 1D-F) (Gendron-Maguire et al., 1993; Rijli et al., 1993). By contrast, ectopic expression of *Hoxa2* in CNCCs (the NCC-*Hoxa2* mouse) results in duplication of skeletal elements derived from PA2, such as the stapes, styloid process and pinna, in the PA1 region, as well as complete loss of the EAM and tympanic ring (Kitazawa et al., 2015b; see also Minoux et al., 2013). Furthermore, although it was formerly generally believed that the EAM invaginates at the first pharyngeal cleft, which is the groove located at the interface between PA1 and PA2 (Grevellec and Tucker, 2010; Jakubíková et al., 2005; Schoenwolf and Larsen, 2009), the mouse EAM has been found to originate in PA1 territory (Minoux et al., 2013). Therefore, in the mouse both the EAM and tympanic ring are considered to derive from PA1, and PA1 is crucial for TM formation.

An analysis that is analogous to establishing the *Hoxa2* knockout mouse was performed in avian embryos. Noden (1983) grafted the quail neural fold of rhombomere (r) 1-2 from the hindbrain heterotopically into the otic levels of the chick. In the chimera, the PA2 neural crest-derived structures are absent and replaced with PA1 elements; it exhibits a duplicate of the jaw and loss of the columella auris (Noden, 1983; also see Couly et al., 1998). Duplication of an EAM-like structure is also described, suggesting that PA1 plays an important role in EAM formation in the chick, as in the mouse, and that the TM is formed by similar developmental mechanisms in terms of A-P patterning of the PAs in mammals and diapsids. However, detailed analysis of TM formation has not previously been performed in the chick-quail chimera (Noden, 1983).

In this study, we examine EAM and TM formation, focusing on the A-P patterning of the PAs in the mouse and chick. We visualize the boundary between PA1 and PA2 by examining *Hoxa2* expression to compare the position of the forming TM in mouse and chick embryos. We also seek to elucidate differences in the developmental mechanisms of TM formation in the mouse and chick by producing a chick-quail chimera in which PA2 derivatives are transformed into PA1 derivatives. Our data shed light on similarities and differences of the developmental mechanisms of TM formation as well as developmental events which led to differing paths of middle ear evolution in mammals and diapsids.

RESULTS

The entire TM is formed in the PA1 region in the mouse

In the *Hoxa2* knockout mouse, the EAM and tympanic ring, in addition to the malleus and incus, are duplicated in a mirror image of the original components (Rijli et al., 1993) (Fig. 1A-F). In this study, we also confirm that both the original and duplicated EAM attach to PP1, resulting in duplication of the TM at E18.5 in the *Hoxa2* knockout mouse (*Hoxa2*$^{EGFP/EGFP}$; Minoux et al., 2013) (Fig. 1D-F) (also see Mallo and Gridley, 1996). These results strongly suggest that the EAM and tympanic ring derive from PA1, and that in the mouse a PA1-specific genetic program also plays an important role in TM formation (Gendron-Maguire et al., 1993; Rijli et al., 1993). Indeed, the mouse EAM begins to invaginate in PA1 territory (Minoux et al., 2013), but whether the TM also forms in PA1 has not been directly examined. In addition, as the original and duplicated EAM-tympanic rings and TMs in the *Hoxa2* knockout mouse are incomplete in shape and size compared with wild type (Fig. 1A,B,D,E), a partial contribution of PA2 mesenchyme to EAM-tympanic ring formation could not be ruled out.

To test this we used the *Hoxa2*$^{EGFP/+}$ mouse as a readout, in which *EGFP* is knocked in at the *Hoxa2* locus and recapitulates *Hoxa2* expression (Fig. 2) (Pasqualetti et al., 2002). We first mapped

Development (2017) 144, 3315-3324 doi:10.1242/dev.149765

the position of the boundary between PA1 and *Hoxa2*$^{EGFP/+}$ PA2 in relation to the development of the TM. We examined aggrecan (*Acan*) expression by *in situ* hybridization to visualize chondrogenesis and checked the anterior boundary of the EGFP signal by immunohistochemistry at E12.5 (Fig. 2A,B). The malleus and incus began forming in the EGFP-negative PA1 area (Fig. 2B), whereas the orbicular apophysis of the malleus (a PA2 derivative; Mason, 2013; O'Gorman, 2005) was located in the EGFP-positive area (Fig. 2B). Thus, the anterior border of EGFP expression domain can be referred to as the boundary between PA1 and PA2 (Minoux et al., 2013). The apex of the EAM was positioned in PA1 territory at E12.5 (Fig. 2C) (Minoux et al., 2013). At E14.5, PA2 derivatives, such as the styloid process, were included in the EGFP-positive area, whereas PA1 derivatives such as the tympanic ring were mapped in the PA1 region (Fig. 2D). The whole TM was formed in PA1 territory (Fig. 2D). We further confirmed that the forming tympanic ring and TM were generated in the PA1 region in the E14.5 and E16.5 *R4::Cre;Rosa-CAG-LSL-tdTomato* mouse, in which the CNCCs in PA2 are labeled by tdTomato (Fig. S1). In the E18.5 *Hoxa2*$^{EGFP/+}$ mouse, PA2 derivatives, such as the orbicular apophysis and the styloid process, were still labeled with EGFP (Fig. 2E). We reconstructed the middle ear region based on consecutive histological sections of the E18.5 *Hoxa2*$^{EGFP/+}$ fetus after EGFP immunohistochemistry. The majority of the EAM, tympanic ring and TM were found in the EGFP-negative PA1-derived territory (Fig. 2F).

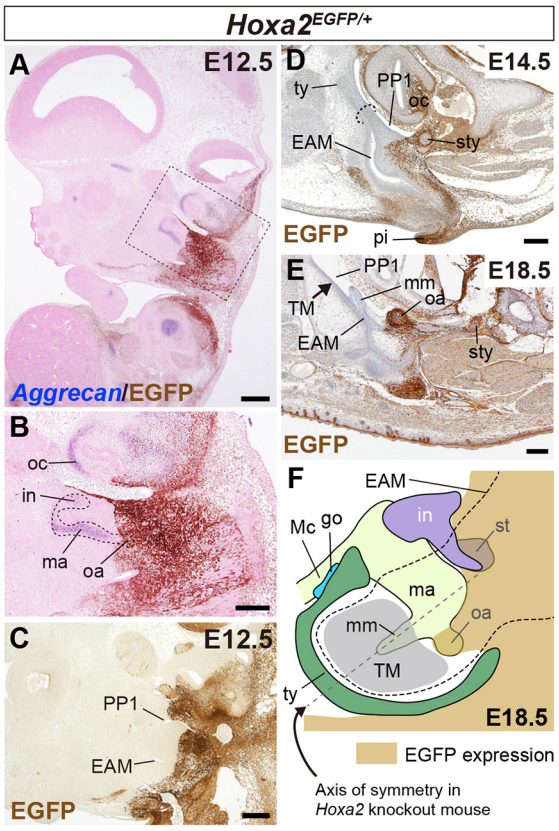

Fig. 2. EGFP expression in the middle ear region of the *Hoxa2*$^{EGFP/+}$ mouse embryo. (A,B) *In situ* hybridization of *Acan* (blue) and immunohistochemistry of EGFP (brown) in a sagittal section at E12.5. (B) Higher magnification of the boxed region in A. (C) EGFP expression in a sagittal section at E12.5. (D,E) EGFP expression in horizontal sections corresponding to the TM level of E14.5 (D) and E18.5 (E) mouse embryos. Dotted line in D indicates the plane of the future TM. (F) Schematic of the middle ear in an E18.5 *Hoxa2*$^{EGFP/+}$ mouse embryo. The brown area indicates the EGFP expression domain in the TM formation region. Mc, Meckel's cartilage; oa, orbicular apophysis; oc, otic capsule; pi, pinna (for other abbreviations see Fig. 1). Scale bars: 200 µm, except 500 µm in A.

Detailed analysis of chicken TM development

We next investigated EAM and TM formation in chick embryos. In E5 and E6 embryos, three hillocks on each side of the first pharyngeal cleft were detected (a-c and d-f, Fig. 3A,B) (Moldenhauer, 1877; Hamburger and Hamilton, 1951). We examined the relative positions of the boundary between PA1 and PA2 and of invagination of the EAM using the *Hoxa2* expression pattern visualized by *in situ* hybridization. The anterior end of the *Hoxa2* expression domain corresponded to PP1 at E6 (data not shown) and E7 (Fig. 3G) and can thus be referred to as the boundary between PA1 and PA2. The first developmental event of EAM formation was an invagination of the surface ectoderm at the depressed area of hillock 'e' in the E6 embryo (Fig. 3B,F). This first invagination was detected in the *Hoxa2* expression domain, namely the PA2 territory (Fig. 3F). Subsequently, the growing apex of the EAM traveled caudally in the PA2 area at E7 and E8 (Fig. 3C,D,G,H), and formed the TM by attaching to PP1 at E10 (Fig. 3E,I). Three-dimensional (3D) reconstruction of the jaw and middle ear based on consecutive histological sections of the E11 embryo showed that the EAM was associated with the forming columella auris, sandwiching the PP1-derived middle ear cavity to form the TM (Fig. 3L,M). At this stage, *Hoxa2* expression was still detected in the region where PA2 derivatives, such as the columella auris and connective tissue of the mandibular depressor muscle, form (Fig. 3J,K). Importantly, we found that the mesenchyme located between the EAM and PP1 expressed *Hoxa2* at E10 and E11 (Fig. 3I,K). We identified the boundary between PA1 and PA2 based on consecutive histological sections showing *Hoxa2* expression at E11, and found that the entire forming TM was entirely encompassed within the *Hoxa2* expression domain (Fig. 3L, yellow dotted line).

To confirm that the *Hoxa2* expression pattern at E11 marks the PA2 region, we also performed cell lineage tracing analysis by producing chick-quail chimeras (Fig. S2). The left side of the neural fold that gives rise to CNCCs migrating into PA2 (r4 together with a portion of r3 and r5; Kulesa and Fraser, 2000) was excised from the Hamburger and Hamilton (HH) stage 9 chick embryo, and the corresponding area in a quail embryo was orthotopically transplanted (Fig. S2A). The transplanted quail cells were identified by QCPN immunohistochemistry at E11 (n=2). We found that the quail cells in the chimeras mostly distributed in the same manner as *Hoxa2*-expressing cells around the TM-forming region (Fig. S2C, D, compare with Fig. 3J,K). The intense signals of *Hoxa2* expression correspond to a high density of QCPN-positive cells (Fig. 3K, Fig. S2D). The mesenchymal cells in the TM were QCPN positive (Fig. S2C,D). These findings collectively indicate that the TM in the chick develops in the PA2 region.

We also found that a depression formed near the EAM opening on the outside surface of the body (Fig. 3E). It was located in PA1 territory, the *Hoxa2*-negative mesenchymal region (Fig. 3E and arrowheads in Fig. 3I,J). Based on these results, the chick EAM can be divided into two parts: the depression of the skin in the PA1 region; and the meatus contributing to the TM in the PA2 region. In this study, these components are referred to as the wall part of the EAM (wEAM) and the TM part of the EAM (tEAM), respectively (Fig. 3E,L-N). These two EAM parts were still observed in the postnatal chick (Fig. 3O). Interestingly, the wEAM was located near the otic process of the quadrate (Fig. 3L).

Development (2017) 144, 3315-3324 doi:10.1242/dev.149765

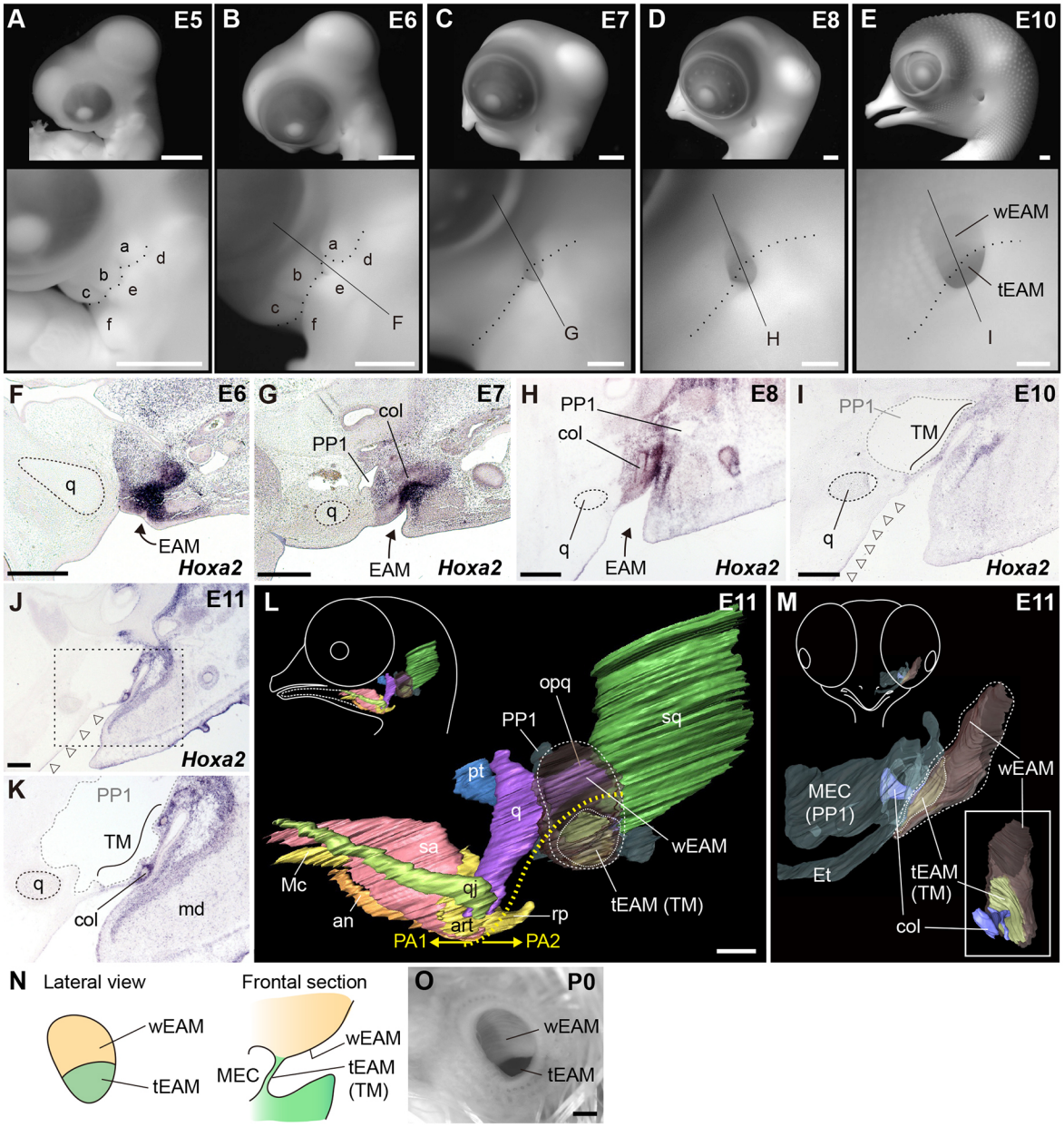

Fig. 3. EAM and TM development in the chick. (A-E) EAM formation in E5-10 chick embryos in lateral view. The heads of chick embryos (top row) and higher magnification of the ear region (bottom row) are shown. a-f indicate the six hillocks seen in PA1 and PA2. Dotted lines indicate the boundary between PA1 and PA2 based on consecutive histological sections of *Hoxa2* expression. (F-I) *In situ* hybridization of *Hoxa2* expression in the ear region of E6-10 chick embryos (planes of section indicated in B-E). (J) *Hoxa2* expression of a frontal section at E11. (K) Higher magnification of the boxed region in J. Arrowheads (I,J) indicate the wEAM in the PA1 region. (L,M) 3D reconstruction of forming TM in an E11 embryo in lateral view (L), frontal view (M) and medial view (box in M). The yellow dotted line in L indicates the boundary between PA1 and PA2 based on consecutive histological sections of *Hoxa2* expression. (N) Schematic of the wEAM and tEAM in the E11 chick embryo in lateral view and a frontal section. (O) The EAM in the postnatal (P0) chick in lateral view. The feathers around the EAM were removed. an, angular; art, articular; col, columella auris; Et, Eustachian tube; md, mandibular depressor muscle; MEC, middle ear cavity; opq, otic process of the quadrate; PA1, first pharyngeal arch; PA2, second pharyngeal arch; pt, pterygoid; q, quadrate; qj, quadratojugal; rp, retroarticular process; sa, surangular; sq, squamosal; tEAM, TM part of the EAM; wEAM, wall part of the EAM (for other abbreviations see Figs 1 and 2). Scale bars: 500 µm, except 2 mm in A-E top and 1 mm in A-E bottom.

Taking these findings together, we found that the chick EAM does not begin to develop from the surface ectoderm at the first pharyngeal cleft, but from the ectoderm in the PA2 region (Fig. 3F), and the entire developing TM is housed in PA2 territory (Fig. 3L,M). These results contrast with mouse TM formation, in which the EAM begins to develop from the ectoderm in the PA1 region (Minoux et al., 2013), and the developing TM is located at PA1 (Fig. 2).

PA2 is necessary for chick TM formation

The fact that the chick TM is formed in PA2 territory suggests that PA2 plays a crucial role in TM development in the chick. To test this, we attempted to generate a chick-quail chimera that exhibits loss of PA2 identity and duplication of PA1 derivatives, as performed by Noden (1983). The neural fold that gives rise to the CNCCs migrating into PA2 was excised from the HH9 chick embryo, and the neural fold corresponding to the midbrain-

Development (2017) 144, 3315-3324 doi:10.1242/dev.149765

hindbrain boundary (MHB) in the HH9 quail embryo was heterotopically transplanted (Fig. 4A). Since CNCCs derived from the transplanted quail graft do not express *Hoxa2*, even when transplanted heterotopically (Couly et al., 1996), the CNCCs should exert a developmental program for establishing PA1 identity in the transplanted location. We confirmed that in the chimera the majority of the CNCCs in PA2 of the operated side were replaced by QCPN-positive quail cells, but the mesodermal cells, distributed in

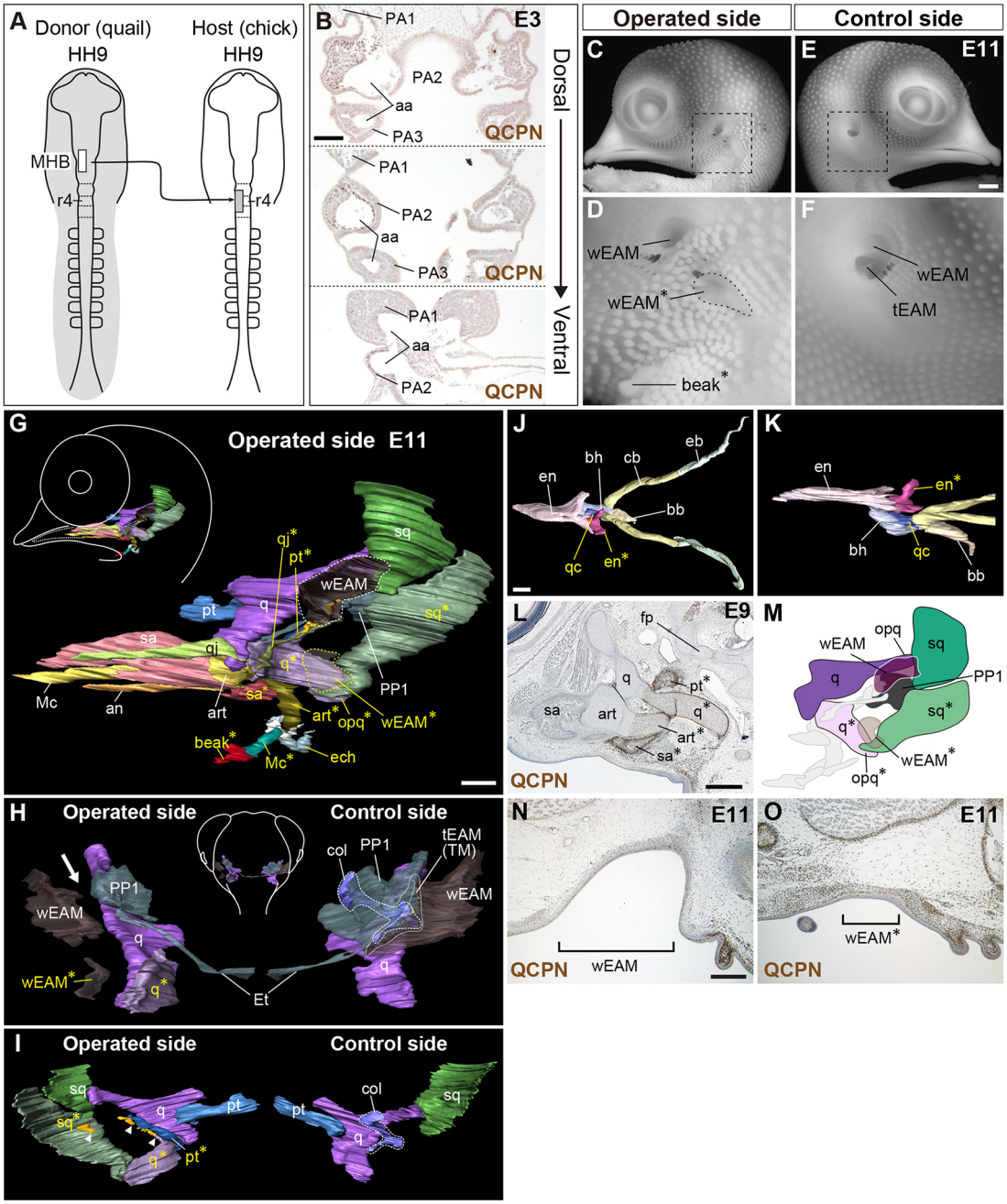

Fig. 4. Detailed phenotype of the chick-quail chimera. (A) Schematic of the chick-quail chimera experiment. (B) Distribution of quail cells in PA2 of the chick-quail chimera at E3. QCPN immunohistochemistry of three different horizontal levels from dorsal (top) to ventral (bottom) PA in a chimera are shown. (C-F) Surface observation of the operated side (C,D) and control side (E,F) in the chimera at E11. (D,F) Higher magnifications of the boxed regions in C and E. (G) 3D reconstruction of the operated side of an E11 chimera from consecutive histological sections. An ectopic cartilage connecting to the hyoid bone is seen (ech). (H) The middle ear in the operated side (left) and control side (right) in dorsal view of the chimera shown in G. The wEAM and PP1 do not contact each other on the operated side (arrow). (I) Ectopic cartilages (orange) and surrounding skeletal components of the operated side (left) and control side (right) in medial view. Arrowheads indicate fusion between the ectopic cartilages and duplicated skeletal elements. (J,K) The hyoid bone of the chimera shown in G in horizontal (J) and lateral (K) view. (L) QCPN immunohistochemistry of a sagittal section in the E9 chimera. (M) Schematic of the middle ear region in the operated side of the chimera shown in G. (N,O) QCPN immunohistochemistry of horizontal sections in the planes of wEAM (N) and wEAM* (O). Asterisks indicate duplicated structures. aa, arch artery; bb, basibranchial; bh, basihyal; cb, ceratobranchial; eb, epibranchial; ech, ectopic cartilage connected to the hyoid bone; en, entoglossum; fp, footplate of the columella auris; PA3, third pharyngeal arch; qc, quail cell contributing to basihyal (for other abbreviations see Figs 1-3). Scale bars: 100 µm in B; 200 µm in E,J,N; 500 µm in G,L.

Development (2017) 144, 3315-3324 doi:10.1242/dev.149765

the lateral area of the arch artery, were derived from QCPN-negative chick cells (Fig. 4B). We collected the chimeras at E9-12 (n=5). The operated side of the chimera exhibited an ectopic beak, as in previous reports (n=4; Fig. 4C-F) (Noden, 1983). 3D reconstruction of consecutive histological sections of the chimeras showed that the endochondral components of the jaw, such as the quadrate, Meckel's cartilage and articular, together with intramembranous components, such as the squamosal, quadratojugal and surangular, were duplicated in a mirror image of the original components (n=5; Fig. 4G, compare with Fig. 3L).

Most of the duplicated and ectopic skeletal elements were derived from QCPN-positive quail cells (Fig. 4L), although a portion of the quadrate included QCPN-negative chick cells. This might be because the boundary between PA1 and PA2, which is normally constructed when CNCCs are migrating, was not established in the chimera and so the CNCCs in these PAs intermingled to some extent.

The columella auris was not formed on the operated side in all chimeras (n=5; Fig. 4H), although the footplate of the columella auris, which is considered to derive from mesoderm (Noden, 1986; Köntges and Lumsden, 1996), was detected in one chimera (Fig. 4L). Interestingly, as Noden (1983) described, ectopic cartilages were detected near the area where the columella auris is normally formed (n=5; Fig. 4I). These ectopic cartilages derived from both QCPN-positive and QCPN-negative cells (data not shown). The cartilages were fused with the duplicated quadrate, pterygoid or squamosal, which are skeletal elements that the columella auris is not connected to in normal development (Fig. 4I), and they were not considered to be portions of the original columella auris.

We further examined the hyoid region in the E11 and E12 chimeras, in which the hyoid bones were well formed (n=4). The entoglossum, a PA1 derivative (Couly et al., 1996), was duplicated on the operated side in all chimeras (Fig. 4J,K). However, the proximal part of the basihyal, a PA2 derivative (Couly et al., 1996), did not disappear and exhibited normal development (Fig. 4K). We also found that QCPN-positive quail cells contributed to the operated side of the basihyal in all chimeras (Fig. 4J,K, qc). From these results, it is likely that although the transplanted quail CNCCs migrated into the original PA2 territory on the operated side, normal chick cells migrating from the control side were able to exert normal development of the basihyal at the midline of the embryo even in the presence of the quail cells. Taken together, the phenotypes detected in the jaw and hyoid regions described above clearly showed that the PA2 derivatives were transformed into PA1 components in the chimeras.

The original EAM on the operated side is much smaller than that of the control side (n=5; Fig. 4D,F). The smaller EAM was formed in proximity to the otic process of the original quadrate (Fig. 4G,M), in PA1 territory where the mesenchyme is composed of QCPN-negative chick cells (Fig. 4N). Therefore, this incomplete EAM appeared to correspond to the wEAM (Fig. 4D,F). 3D reconstruction of consecutive histological sections of the E11 chimeras revealed that the wEAM and PP1 did not contact each other, resulting in an absence of TM formation (n=5; Fig. 4H, arrow).

In addition to formation of only the wEAM part of the original EAM, we found an ectopic depression without feathering at the caudal area of the original EAM position (n=4; Fig. 4D), as described by Noden (1983). The depression formed in the region occupied by QCPN-positive mesenchymal cells (Fig. 4O). Furthermore, the ectopic depression exhibited the morphology of the quail wEAM, with a teardrop shape (n=2; Fig. 4D, Fig. S3). Since CNCCs can impose species-specific morphology on the epithelium (Schneider and Helms, 2003), these results indicate that the ectopic depression was formed by inductive signaling from the transplanted quail CNCCs. On the control side, feathering was not seen on the skin around the tEAM (Fig. 4F), but ectopic feathers surrounded the ectopic depression on the operated side, as in the original wEAM (Fig. 4D, Fig. S3). Importantly, the depression was located in the proximity of the duplicated otic process of the quadrate (Fig. 4G,M), suggesting that it is a duplicated structure corresponding to the wEAM. Taking these findings together, it is reasonable to think that the tEAM was lost and the wEAM was duplicated in the chimera. These results strongly suggest that specific genetic programs in PA1 and PA2 are involved in the wEAM and tEAM, respectively, and thus PA2 plays a crucial role in TM formation in the chick.

DISCUSSION

Evolution of the jaw and middle ear in mammals includes substantial morphological changes, which have attracted considerable research interest (e.g. Takechi and Kuratani, 2010). We propose that the key to understanding the evolution of the middle ear lies in developmental relationships between the TM and skeletal elements (Takechi and Kuratani, 2010; Kitazawa et al., 2015a). We have reported non-homology of the TM in mammals and diapsids (Kitazawa et al., 2015a). In addition, contrary to the classical view, we found that the mouse EAM begins to form at the surface ectoderm in the PA1 region (Minoux et al., 2013). These previous findings prompted us to perform a more detailed comparative analysis of TM formation, especially focusing on A-P patterning of the PAs in mouse and chicken embryos. Our present data suggest that a PA1-specific genetic program plays a crucial role in the formation of the TM in the mouse. By contrast, in the chick, a PA2-specific genetic program is necessary for TM formation, albeit with a certain contribution from PA1 to a portion of EAM formation. Furthermore, we propose that in the chick, the PA2 parts of the EAM and the columella auris are interdependent in TM development, as in the relationship between the EAM and tympanic ring in the mouse.

The mouse TM is a PA1 derivative

In this study we mapped the relative position of the TM with respect to the boundary between PA1 and PA2 territories using the *Hoxa2*$^{EGFP/+}$ knock-in mouse as a readout (Fig. 2). We found that the TM and tympanic ring are formed in the EGFP-negative PA1 territory (Fig. 2F, Fig. 5A) (Minoux et al., 2013), strongly suggesting that the TM is induced by a PA1-specific genetic program in the mouse.

Since, in the *Hoxa2* knockout mouse, PA1 derivatives are duplicated in a mirror-image manner (Fig. 1D-F), patterning signals determining the morphological identity of PA1 derivatives might be provided by PP1, which is located between PA1 and PA2 (Rijli et al., 1993; Mallo, 2001). Based on the phenotype of the *Hoxa2* knockout mouse, the axis of symmetry of the mirror-image duplication lies on the manubrium of the malleus (Fig. 1D,E, Fig. 2F). By contrast, the normal EAM-tympanic ring is formed towards a posterior region of the axis and lateral to the region of the malleus and incus in the wild-type embryo (Fig. 1A,B, Fig. 2F). Thus, it is reasonable to propose that, in the *Hoxa2* knockout mouse, the developing original and duplicated EAM-tympanic rings might interfere with each other, resulting in failure to form the posterior aspect of the components and consequent deficiencies in their shape and size (Fig. 1D,E, Fig. 5B).

Development (2017) 144, 3315-3324 doi:10.1242/dev.149765

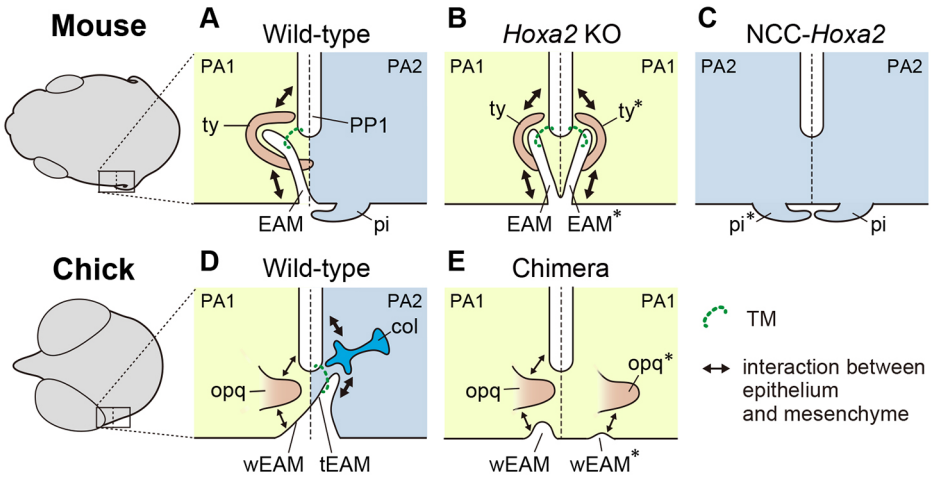

Fig. 5. Comparison of TM development in the mouse and chicken. Schematic of proposed TM development in the wild-type mouse (A), *Hoxa2* knockout mouse (B), NCC-*Hoxa2* mouse (ectopic expression of *Hoxa2* in CNCCs) (C), wild-type chick (D) and chick-quail chimera (E). (A) In the mouse, the TM and tympanic ring are formed in PA1. The main tissue interactions occur between the forming EAM, tympanic ring, and PP1. (B) The *Hoxa2* knockout mouse exhibits duplicated PA1 identity. The TM is duplicated, but development of the posterior part of the EAM-tympanic ring is prevented by PA1 duplication. (C) The NCC-*Hoxa2* mouse shows duplication of pinna but fails to form the EAM-tympanic ring. (D) In the chick, the TM is entirely housed in PA2. The main tissue interactions occur between tEAM, columella auris, and PP1. In addition, the otic process of the quadrate appears to induce the wEAM. (E) The chick-quail chimera exhibits duplication of PA1 identity, and a duplicated wEAM is generated, probably due to duplication of the otic process of the quadrate. Green dotted lines indicate the plane of the future TM.

PA2 is necessary for TM formation in the chick, but PA1 is also involved in EAM formation

We found that the chick EAM begins to invaginate at the PA2 ectoderm and grows directly toward the columella auris in the PA2 region, and a portion of the EAM is also seen in the PA1 region (Fig. 3, Fig. 5D). The boundary between PA1 and PA2 appears to be consistent with the morphology of the EAM (Fig. 3). We thus refer to the two components as wEAM and tEAM, respectively. We then produced chick-quail chimeras in which PA2 is transformed into a PA1-like structure, as previously studied (Fig. 4) (Noden, 1983; Couly et al., 1998). The chimera lost the columella auris and lacked the TM (Fig. 4H). These results suggest that tEAM formation in the chick is largely dependent on a PA2-specific genetic program, and the formation processes of the tEAM and columella auris are interdependent during development, as in the relationship between the EAM and tympanic ring in the mouse (Fig. 5A,D). We also found that wEAM was duplicated in the chimeras, suggesting that wEAM formation is dependent on a PA1-specific genetic program (Fig. 5D,E).

Middle ear development is achieved by interaction between epithelia (PP1 and EAM) and mesenchyme (CNCCs) (Mallo, 2001, 2003). In the chick, the tEAM contacts the columella auris, which mostly derives from the PA2 CNCCs. Therefore, it is likely that interaction between the surface ectoderm and CNCCs in PA2 is important as a primary step of TM formation in the chick (Fig. 5D). Similarly, mesenchyme that generates the otic process of the quadrate appears to be related to wEAM formation (Fig. 5D,E). Since the surface ectoderm in the PA2 territory is not replaced by quail cells in the chimera (Fig. 4B), the mesenchyme that forms the otic process of the quadrate appears to be crucial for initiation of wEAM formation. It is worth noting that the duplicated EAM is a shallow depression, less developed than the original (Fig. 4D,N,O). This difference might be because growth of the wEAM also requires a developmental signal from PP1, and the duplicated wEAM was far from PP1 and unable to receive the signal (Fig. 4G,M, Fig. 5E).

In this study, we did not try to examine avian embryos that exhibit loss of PA1 identity, but rather duplication of PA2, because previous studies have shown that it is difficult to obtain such avian embryos by experimental manipulation. The chick-quail chimera in which the neural crest at the PA1 level (r1-2 or mesencephalon) is transposed to the PA2 level (r4-6) fails to transform PA1 into PA2 identity and results in formation of a normal jaw (Couly et al., 1998). This is because the Hox-negative CNCCs derived from rostral to the r1-2 area compensate for the lost area of the neural crest (Couly et al., 1998). When the broad area from the forebrain to hindbrain level is ablated in chick, and the quail r4-6 level is transplanted, the embryo exhibits loss of the jaw structure, but duplication of PA2 identity is not observed (Couly et al., 1998). Similarly, when a retroviral vector or active virus that expresses *Hoxa2* ectopically is introduced to the chick, the jaw structure is lost but duplication of the columella auris does not occur (Grammatopoulos et al., 2000). Thus, further experimental modification might be needed to confirm whether the columella auris and tEAM are duplicated when PA2 is duplicated and PA1 is lost in avian embryos.

Comparison of TM formation in mammals and diapsids

In contrast to the traditional view, our present data suggest that the EAM does not begin to form at the first pharyngeal cleft in either mouse or chick (Fig. 5A,D). The traditional view postulated that signals derived from the interface of PA1 and PA2 are involved in EAM formation, but our data suggest that such signals are not relevant to the beginning of EAM formation. However, although the EAM does not invaginate at the boundary between PA1 and PA2, in the chick the EAM straddles both PA1-derived and PA2-derived territories (Fig. 5D). Interestingly, the boundary between PA1 and PA2 may partition the chick EAM into its components, namely the wEAM and tEAM (Fig. 3). Since both PA1 and PA2 are involved in EAM formation in the chick (Fig. 4), the developmental mechanisms of EAM formation might utilize the interface of the PA1 and PA2 to generate morphological differences. These constitute differences to mouse external and middle ear development: only PA1 contributes to EAM and TM formation, whereas PA2 is involved in pinna formation in mouse (Fig. 5B,C) (Kitazawa et al., 2015b; Minoux et al., 2013; Rijli et al., 1993). It

Development (2017) 144, 3315-3324 doi:10.1242/dev.149765

will be of interest to elucidate if other diapsid species also exhibit EAM-TM formation similar to the chick embryo.

We found that the TM is formed in PA1 in the mouse, but the entire TM is housed in the PA2 region in the chick (Figs 2 and 3). Therefore, regional contributions of PP1 to the TM may differ between mouse and chick; the contribution of PP1 in the PA2 territory is much larger in the chick than in the mouse (Fig. 5A,D). Although the prevailing view has been that PP1 is a comparable component for TM formation in mammals and diapsids, our observation suggests that different PP1 regions along the A-P axis contribute to the TM in these animals. In this regard, the epithelium of the middle ear cavity appears to originate from both endoderm and CNCCs in mammals, but not in diapsids (Thompson and Tucker, 2013). Future study elucidating the precise regional contribution of PP1 to the TM during mouse and chick development will be needed in order to provide further insight into the differences in TM formation in these lineages.

Loss of PA2 and duplication of PA1 results in duplication of the EAM in mouse and chick (Noden, 1983; Rijli et al., 1993), suggesting that PA1 is crucial for TM formation in both animals. However, we found that the original and duplicated EAMs form the TMs in the mouse (Fig. 5B) but not in the chick (Fig. 5E). Our findings suggest that TM formation in the mouse is highly dependent on a PA1-specific genetic program, whereas the chick TM is associated with a PA2-specific genetic program. Since the EAM finally reaches PP1 to form the TM, signals induced from PP1 to the surface ectoderm might be involved in TM formation. However, previous reports in mouse (Mallo et al., 2000; Mallo and Gridley, 1996; Yamada et al., 1995) and our present data in chick (Fig. 4) suggest that one of the main interactions for TM formation between epithelium and mesenchyme occurs between the cells that give rise to the EAM and tympanic ring (a PA1 derivative) in mammals, but the EAM and columella auris (a PA2 derivative) in diapsids. Therefore, it is likely that the EAM begins to form in proximity to the skeletal component in the PA1 region in mouse but in the PA2 region in chick. The tympanic ring and columella auris are a lower jaw and an upper jaw component, respectively. The idea of a close relationship between the EAM and these skeletal elements supports our previous report that the TM is formed as a lower jaw component by Edn1 signaling in mammals, but as an upper jaw component in diapsids (Kitazawa et al., 2015a).

The present study shows that although developmental interactions between epithelium and mesenchyme are crucial for TM formation in both mammals and diapsids, one of the main interactions appears to occur with different developmental origins in different PAs in these lineages. Further research should elucidate precisely how amniotes independently evolved functionally similar systems with different developmental origins and mechanisms.

MATERIALS AND METHODS

Sample collection

Hoxa2$^{EGFP/EGFP}$, *Hoxa2*$^{EGFP/+}$ and *R4::Cre;Rosa-CAG-LSL-tdTomato* mice (*Mus musculus*) were described previously (Minoux et al., 2013; Pasqualetti et al., 2002). These transgenic and ICR mice were housed in an environmentally controlled room at 23±2°C, under a 12-h light:12-h dark cycle. Embryos were staged according to Theiler (1989). Fertilized eggs of the chicken *Gallus gallus domesticus* and quail *Coturnix coturnix japonica* were incubated at 38°C and staged according to Hamburger and Hamilton (1951). Animal care was entirely in accordance with the guidelines provided by the Tokyo Medical and Dental University, The University of Tokyo, and Friedrich Miescher Institute for Biomedical Research, and approval for the experiments was obtained from the institutions.

Histological analysis

Embryos of wild-type and *Hoxa2* knockout mice were fixed with Bouin's fixative overnight at room temperature (RT), dehydrated, penetrated by xylene, and embedded in paraffin. The samples were cut into 8 µm horizontal (transverse) sections. The sections were stained with Hematoxylin and Eosin.

In situ hybridization

Digoxigenin (DIG)-labeled riboprobes for mouse *Acan* and chick *Hoxa2* were generated using the DIG RNA Labeling Kit (Roche) based on GenBank nucleotide sequences NM_007424 and NM_205150, respectively. *Hoxa2*$^{EGFP/+}$ mouse embryos were fixed with Carnoy's fixative overnight at RT. Chick E6 and E7 embryos were fixed with 4% paraformaldehyde (PFA) in PBS overnight (or for ∼2 days) at RT. The samples were then dehydrated, penetrated by xylene, and embedded in paraffin. Chick E8, E10 and E11 embryos were directly embedded in O.C.T. compound (Sakura Finetek) without fixation. These samples were sliced into 8-16 µm horizontal (transverse) or frontal (coronal) sections.

A Ventana Discovery XT system (Roche-Ventana Medical Systems) was used to perform *in situ* hybridization for mouse *Acan*. *In situ* hybridization for chick *Hoxa2* was performed as previously described (Schaeren-Wiemers and Gerfin-Moser, 1993; Sockanathan, 2015) with slight modifications. Briefly, the sections were fixed in 4% PFA in PBS for 5-10 min followed by 10 min acetylation (21 µM HCl, 100 µM triethanolamine in water, 0.25% acetic anhydride) at RT. The sections were hybridized with hybridization buffer (50% formamide, 10 mM Tris HCl pH 7.6, 200 µg/ml *E. coli* tRNA, 1× Denhardt's solution, 5% dextran sulfate, 600 mM NaCl, 0.25% SDS, 1 mM EDTA) with riboprobe overnight at 70°C. The hybridized sections were incubated with anti-DIG antibody (Roche, 11093274910; 1/5000) overnight at 4°C. DIG was detected by nitro blue tetrazolium chloride (NBT)/5-bromo-4-chloro-3-indolyl phosphate (BCIP) (Roche). The sections were detected using a lightfield microscope (Olympus BX50) with a camera system (Olympus DP80).

Immunohistochemistry

Hoxa2$^{EGFP/+}$ and *R4::Cre;Rosa-CAG-LSL-tdTomato* mouse embryos and chick-quail chimera embryos were fixed with Carnoy's fixative overnight (or for ∼2 days) at RT, then dehydrated, penetrated by xylene, and embedded in paraffin. The samples were sliced into 8-10 µm horizontal or sagittal sections, which were then treated with 0.3% or 3% H_2O_2 in methanol for 20 min. For detection of EGFP or tdTomato, activation of antigen in sodium citrate buffer (1.8 µM citric acid monohydrate, 8.2 µM trisodium citrate dihydrate) at 97°C for 20-40 min was performed. The sections were incubated with anti-GFP antibody (ab6673, Abcam; 1:500), anti-RFP antibody (600-401-379, Rockland; 1/1000 or 1/2000) or QCPN antibody (Developmental Studies Hybridoma Bank; 1:10). The sections were then incubated with secondary antibody conjugated with biotin (Vector Laboratories; 1:500) for 30 min, followed by avidin-biotin complex (Vector Laboratories, Vectastain Elite ABC Kit; 1/100) for 30 min, and visualized using the Metal-Enhanced DAB Substrate Kit (Thermo Fisher Scientific). Counterstaining was performed with Hematoxylin. The sections were detected using the BX50-DP80 system.

Chick-quail chimeras

Chick embryos at HH9 were prepared for *in ovo* surgery. The left side of r4 together with a portion of r3 and r5, which constitutes the PA2-forming level of the hindbrain crest (Kulesa and Fraser, 2000), was ablated from the chick with a tungsten needle. The stage-matching quail embryos were obtained as donors, and the left side of the neural crest corresponding to the ablated region of the chick or to MHB was isolated with a tungsten needle in sterile saline. The isolated graft was transplanted into the ablated region of the chick host (Fig. S2A, Fig. 4A). Chimeric embryos were incubated at 38°C and collected at E3-12. The unoperated right-hand side was used as a control in this chimera experiment. Imaging of the whole-mount samples was by stereoscopic microscope (Olympus SZX16) with DP80.

Development (2017) 144, 3315-3324 doi:10.1242/dev.149765

3D reconstruction

Consecutive histological sections after staining were recorded with the BX50-DP80 system. The images of the sections were reconstructed with Avizo v6.3 (FEI).

Acknowledgements

We thank Tatsuya Hirasawa and Sachiko Miyagawa-Tomita for helpful discussion; Norisuke Yokoyama, Jie Gu and Miyuri Kawasumi for helpful support; and Maryline Minoux for valuable comments on the manuscript.

Competing interests

The authors declare no competing or financial interests.

Author contributions

Conceptualization: M.T., T.K., F.M.R., H.K., S.K., S.I.; Methodology: M.T., T.F., T.K., S.I.; Validation: M.T., T.F., J.T., T.Y.; Investigation: M.T., T.F., J.T., T.Y., T.V.; Resources: M.T., T.F., T.K., F.M.R.; Writing - original draft: M.T., T.F.; Writing - review & editing: M.T., T.K., F.M.R., S.I.; Visualization: M.T., T.F.; Supervision: M.T., S.I.; Project administration: M.T., S.I.; Funding acquisition: M.T., T.K., F.M.R., S.I.

Funding

This work was supported by grants-in-aid from the Ministry of Education, Culture, Sports, Science, and Technology of Japan [26460256 to M.T., 16K15746 to S.I.] and Takeda Science Foundation, Osaka, Japan to M.T. T.K. is supported by a Japan Society for the Promotion of Science Overseas Research Fellowship, and F.M.R. is supported by the Swiss National Science Foundation [Schweizerischer Nationalfonds zur Förderung der Wissenschaftlichen Forschung; 31003A_149573] and Novartis Foundation.

Supplementary information

Supplementary information available online at
http://dev.biologists.org/lookup/doi/10.1242/dev.149765.supplemental

References

Anthwal, N., Joshi, L. and Tucker, A. S. (2013). Evolution of the mammalian middle ear and jaw: adaptations and novel structures. *J. Anat.* **222**, 147-160.

Chapman, S. C. (2011). Can you hear me now? Understanding vertebrate middle ear development. *Front. Biosci. (Landmark Ed)* **16**, 1675-1692.

Chin, K., Kurian, R. and Saunders, J. C. (1997). Maturation of tympanic membrane layers and collagen in the embryonic and post-hatch chick (Gallus domesticus). *J. Morphol.* **233**, 257-266.

Clack, J. A. (2002). *Gaining Ground. The Origin and Evolution of Tetrapods*. Bloomington, Indianapolis: Indiana University Press.

Clack, J. A. and Allin, E. F. (2004). The evolution of single- and multiple-ossicle ears in fishes and tetrapods. In *Evolution of the Vertebrate Auditory System* (ed. G. A. Manley, A. N. Popper and R. R. Fay), pp. 128-163. New York: Springer.

Clouthier, D. E., Passos-Bueno, M. R., Tavares, A. L. P., Lyonnet, S., Amiel, J. and Gordon, C. T. (2013). Understanding the basis of auriculocondylar syndrome: Insights from human, mouse and zebrafish genetic studies. *Am. J. Med. Genet. C Semin. Med. Genet.* **163C**, 306-317.

Couly, G., Grapin-Botton, A., Coltey, P. and Le Douarin, N. M. (1996). The regeneration of the cephalic neural crest, a problem revisited: the regenerating cells originate from the contralateral or from the anterior and posterior neural fold. *Development* **122**, 3393-3407.

Couly, G., Grapin-Botton, A., Coltey, P., Ruhin, B. and Le Douarin, N. M. (1998). Determination of the identity of the derivatives of the cephalic neural crest: incompatibility between Hox gene expression and lower jaw development. *Development* **125**, 3445-3459.

Fuchs, J. C. and Tucker, A. S. (2015). Development and integration of the ear. *Curr. Top. Dev. Biol.* **115**, 213-232.

Gendron-Maguire, M., Mallo, M., Zhang, M. and Gridley, T. (1993). Hoxa-2 mutant mice exhibit homeotic transformation of skeletal elements derived from cranial neural crest. *Cell* **75**, 1317-1331.

Grammatopoulos, G. A., Bell, E., Toole, L., Lumsden, A. and Tucker, A. S. (2000). Homeotic transformation of branchial arch identity after Hoxa2 overexpression. *Development* **127**, 5355-5365.

Grevellec, A. and Tucker, A. S. (2010). The pharyngeal pouches and clefts: development, evolution, structure and derivatives. *Semin. Cell Dev. Biol.* **21**, 325-332.

Hamburger, V. and Hamilton, H. L. (1951). A series of normal stages in the development of the chick embryo. *J. Morph.* **88**, 49-92.

Jakubíková, J., Staník, R. and Staníková, A. (2005). Malformations of the first branchial cleft: duplication of the external auditory canal. *Int. J. Pediatr. Otorhinolaryngol.* **69**, 255-261.

Kempf, H., Linares, C., Corvol, P. and Gasc, J. M. (1998). Pharmacological inactivation of the endothelin type A receptor in the early chick embryo: a model of mispatterning of the branchial arch derivatives. *Development* **125**, 4931-4941.

Kitazawa, T., Takechi, M., Hirasawa, T., Adachi, N., Narboux-Nême, N., Kume, H., Maeda, K., Hirai, T., Miyagawa-Tomita, S., Kurihara, Y. et al. (2015a). Developmental genetic bases behind the independent origin of the tympanic membrane in mammals and diapsids. *Nat. Commun.* **6**, 6853.

Kitazawa, T., Fujisawa, K., Narboux-Nême, N., Arima, Y., Kawamura, Y., Inoue, T., Wada, Y., Kohro, T., Aburatani, H., Kodama, T. et al. (2015b). Distinct effects of Hoxa2 overexpression in cranial neural crest populations reveal that the mammalian hyomandibular-ceratohyal boundary maps within the styloid process. *Dev. Biol.* **402**, 162-174.

Köntges, G. and Lumsden, A. (1996). Rhombencephalic neural crest segmentation is preserved throughout craniofacial ontogeny. *Development* **122**, 3229-3242.

Kulesa, P. M. and Fraser, S. E. (2000). In ovo time-lapse analysis of chick hindbrain neural crest cell migration shows cell interactions during migration to the branchial arches. *Development* **127**, 1161-1172.

Laurin, M. (1998). The importance of global parsimony and historical bias in understanding tetrapod evolution. Part I. Systematics, middle ear evolution and jaw suspension. *Annales des Sciences Naturelles - Zoologie et Biologie Animale* **19**, 1-42.

Laurin, M. (2010). *How Vertebrates Left the Water*. London: University of California Press.

Lombard, R. E. and Bolt, J. R. (1979). Evolution of the tetrapod ear: an analysis and reinterpretation. *Biological J. Linnean Soc.* **11**, 19-76.

Maier, W. and Ruf, I. (2016). Evolution of the mammalian middle ear: a historical review. *J. Anat.* **228**, 270-283.

Mallo, M. (2001). Formation of the middle ear: recent progress on the developmental and molecular mechanisms. *Dev. Biol.* **231**, 410-419.

Mallo, M. (2003). Formation of the outer and middle ear, molecular mechanisms. *Curr. Top. Dev. Biol.* **57**, 85-113.

Mallo, M. and Gridley, T. (1996). Development of the mammalian ear: coordinate regulation of formation of the tympanic ring and the external acoustic meatus. *Development* **122**, 173-179.

Mallo, M., Schrewe, H., Martin, J. F., Olson, E. N. and Ohnemus, S. (2000). Assembling a functional tympanic membrane: signals from the external acoustic meatus coordinate development of the malleal manubrium. *Development* **127**, 4127-4136.

Manley, G. A. and Sienknecht, U. J. (2013). The evolution and development of middle ears in land vertebrates. In *The Middle Ear: Science, Otosurgery, and Technology* (ed. S. Puria, R. R. Fay and A. N. Popper), pp. 7-30. New York: Springer.

Mason, M. J. (2013). Of mice, moles and guinea pigs: functional morphology of the middle ear in living mammals. *Hear. Res.* **301**, 4-18.

Medeiros, D. M. and Crump, J. G. (2012). New perspectives on pharyngeal dorsoventral patterning in development and evolution of the vertebrate jaw. *Dev. Biol.* **371**, 121-135.

Minoux, M., Kratochwil, C. F., Ducret, S., Amin, S., Kitazawa, T., Kurihara, H., Bobola, N., Vilain, N. and Rijli, F. M. (2013). Mouse Hoxa2 mutations provide a model for microtia and auricle duplication. *Development* **140**, 4386-4397.

Moldenhauer, M. (1877). Die Entwicklung des mittleren und des äußeren Ohres. *Morphol. Jahrb.* **3**, 106-151.

Müller, J. and Tsuji, L. A. (2007). Impedance-matching hearing in Paleozoic reptiles: evidence of advanced sensory perception at an early stage of amniote evolution. *PLoS ONE* **2**, e889.

Noden, D. M. (1983). The role of the neural crest in patterning of avian cranial skeletal, connective, and muscle tissues. *Dev. Biol.* **96**, 144-165.

Noden, D. M. (1986). Origins and patterning of craniofacial mesenchymal tissues. *J. Craniofac. Genet. Dev. Biol. Suppl.* **2**, 15-31.

O'Gorman, S. (2005). Second branchial arch lineages of the middle ear of wild-type and Hoxa2 mutant mice. *Dev. Dyn.* **234**, 124-131.

Ozeki, H., Kurihara, Y., Tonami, K., Watatani, S. and Kurihara, H. (2004). Endothelin-1 regulates the dorsoventral branchial arch patterning in mice. *Mech. Dev.* **121**, 387-395.

Pasqualetti, M., Ren, S.-Y., Poulet, M., LeMeur, M., Dierich, A. and Rijli, F. M. (2002). A Hoxa2 knockin allele that expresses EGFP upon conditional Cre-mediated recombination. *Genesis* **32**, 109-111.

Reichert, K. B. (1837). Über die Visceralbogen der Wirbelthiere im Allgemeinen und deren Metamorphosen bei den Vögeln und Säugethieren. *Arch. Anato. Physiol. Wiss. Med.* **1837**, 120-222.

Rijli, F. M., Mark, M., Lakkaraju, S., Dierich, A., Dollé, P. and Chambon, P. (1993). A homeotic transformation is generated in the rostral branchial region of the head by disruption of Hoxa-2, which acts as a selector gene. *Cell* **75**, 1333-1349.

Ruest, L.-B., Xiang, X., Lim, K. C., Levi, G. and Clouthier, D. E. (2004). Endothelin-A receptor-dependent and -independent signaling pathways in establishing mandibular identity. *Development* **131**, 4413-4423.

Sato, T., Kawamura, Y., Asai, R., Amano, T., Uchijima, Y., Dettlaff-Swiercz, D. A., Offermanns, S., Kurihara, Y. and Kurihara, H. (2008). Recombinase-mediated cassette exchange reveals the selective use of Gq/G11-dependent and -independent endothelin 1/endothelin type A receptor signaling in pharyngeal arch development. *Development* **135**, 755-765.

Development (2017) 144, 3315-3324 doi:10.1242/dev.149765

Schaeren-Wiemers, N. and Gerfin-Moser, A. (1993). A single protocol to detect transcripts of various types and expression levels in neural tissue and cultured cells: in situ hybridization using digoxigenin-labelled cRNA probes. *Histochemistry* **100**, 431-440.

Schneider, R. A. and Helms, J. A. (2003). The cellular and molecular origins of beak morphology. *Science* **299**, 565-568.

Schoenwolf, G. C. and Larsen, W. J. (2009). *Larsen's Human Embryology*, 4th edn. Philadelphia, PA: Elsevier/Churchill Livingstone.

Sockanathan, S. (2015). In situ hybridization of chick and mouse embryonic tissue. *Protocol Exchange*, doi:10.1038/protex.2015.040.

Takechi, M. and Kuratani, S. (2010). History of studies on mammalian middle ear evolution: a comparative morphological and developmental biology perspective. *J. Exp. Zool. B Mol. Dev. Evol.* **314**, 417-433.

Takechi, M., Kitazawa, T., Hirasawa, T., Hirai, T., Iseki, S., Kurihara, H. and Kuratani, S. (2016). Developmental mechanisms of the tympanic membrane in mammals and non-mammalian amniotes. *Congenit. Anom. (Kyoto)* **56**, 12-17.

Theiler, K. (1989). *The House Mouse. Atlas of Embryonic Development*. New York: Springer.

Thompson, H. and Tucker, A. S. (2013). Dual origin of the epithelium of the mammalian middle ear. *Science* **339**, 1453-1456.

Thompson, H., Ohazama, A., Sharpe, P. T. and Tucker, A. S. (2012). The origin of the stapes and relationship to the otic capsule and oval window. *Dev. Dyn.* **241**, 1396-1404.

Wever, E. G. (1978). *The Reptile Ear. Its Structure and Function*. Princeton, New Jersey: Princeton University Press.

Yamada, G., Mansouri, A., Torres, M., Stuart, E. T., Blum, M., Schultz, M., De Robertis, E. M. and Gruss, P. (1995). Targeted mutation of the murine goosecoid gene results in craniofacial defects and neonatal death. *Development* **121**, 2917-2922.

Zou, Y., Mak, S.-S., Liu, H. Z., Han, D. Y., Zhuang, H. X., Yang, S. M. and Ladher, R. K. (2012). Induction of the chick columella and its integration with the inner ear. *Dev. Dyn.* **241**, 1104-1110.

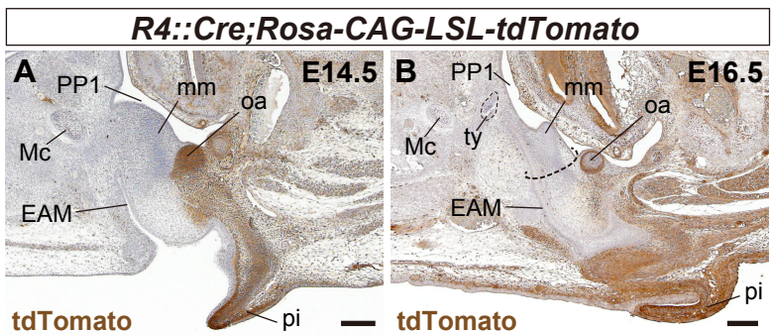

Fig. S1. tdTomato expression in the *R4::Cre;Rosa-CAG-LSL-tdTomato* mouse. The tdTomato expression (brown) in horizontal sections of E14.5 (A) and E16.5 (B) embryos. Dotted line in B indicates the plane of future TM. Scale bars: 200 μm.

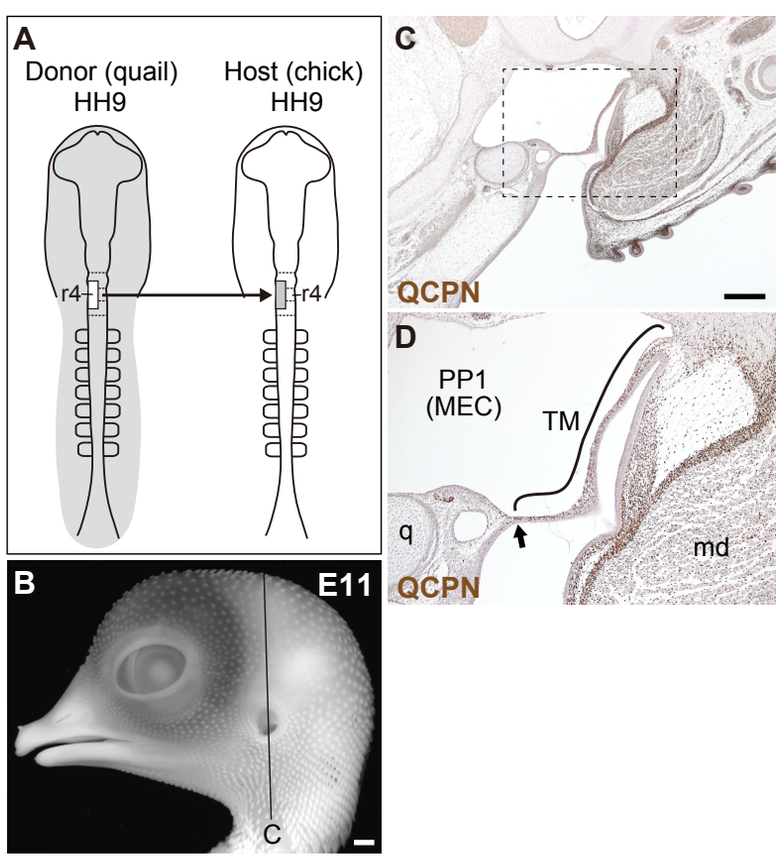

Fig. S2. Identification of the PA1/PA2 boudnary by producing chick-quail chimera. (A) Schematic of the chick-quail chimera experiment. (B) Surface observation of the operated side in the chimera at E11. (C) QCPN immunohistochemistry in the section in the plane of the line indicated in B. (D) Higher magnification of the boxed region in C. Arrow indicates the boundary between QCPN-positive quail cells and QCPN-negative chick cells. Scale bars: 2mm in B, 500 μm in C.

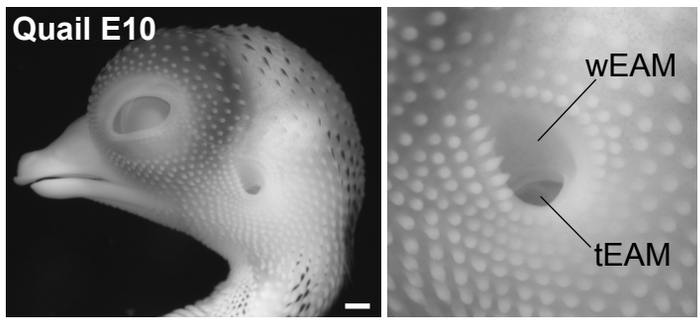

Fig. S3. Morphology of the EAM in the quail embryo. (A) Surface observation of the left side of the E10 quail embryo. (B) Higher magnification of the EAM region. The wEAM exhibits a teardrop shape, which is different from the chick (Fig. 3E). Scale bar: 2mm.